

LIGHT METAL HYDRIDES UNDER NON-AMBIENT CONDITIONS: PROBING CHEMISTRY BY DIFFRACTION?

YAROSLAV FILINCHUK*

*Swiss-Norwegian Beam Lines at the European Synchrotron
Radiation Facility, BP-220, 38043 Grenoble, France*

Abstract Experimental studies of light metal hydrides under variable pressure and temperature are reviewed with an emphasis on the methodological aspects: collecting good quality powder data, solving new structures, relating different polymorphs in an attempt to reveal phase transition mechanisms and the underlying crystal chemistry. Practical recommendations and examples are given.

Keywords: High pressure, synchrotron powder diffraction, structure solution, hydrogen storage, mechanism of phase transition, phase diagram

1. Introduction

Light metal hydrides, such as borohydrides $M(BH_4)_n$, ammonia borane NH_3BH_3 etc. are considered as prospective hydrogen storage materials. Indeed, they can desorb a large quantity of hydrogen (up to 20.8%), that is much higher than traditional transition metal based hydrides, like $LaNi_5H_{5-7}$. However, the decompositon temperatures of borohydrides are usually high and the known compounds do not easily reabsorb hydrogen – thus they lack the reversibility.

Most of the light hydrides are crystalline solids, giving an advantage of using diffraction methods to study their structure and transformations. Diffraction provides an immense amount of information not only about the structure, but also is more and more frequently used for screening and characterization of new substances, reaction products and intermediates. Detailed diffraction study of a promising material at various temperatures and pressures allows to uncover new polymorphs, follow their structural

* E-mail: Yaroslav.Filinchuk@esrf.fr

evolution and therefore understand the nature of the interactions, or more generally speaking the underlying chemistry of the system. This information is a clue to understanding and maybe even altering the thermodynamic stability and reversibility of hydrides.

This chapter will be mostly focused on the high-pressure studies of the light hydrides. Besides showing how to solve new crystal structures, it is also aiming to give a feeling about how much modern diffraction techniques can go beyond a simple structure characterization. High-pressure characterization of the most relevant hydrides, such as LiBH_4 and $\text{Mg}(\text{BH}_4)_2$ (they release hydrogen at rather high T but show some reversibility) and NH_3BH_3 (releases hydrogen already at 80°C but shows no reversibility) is a part of a more common approach, where the changes are monitored under non-ambient conditions – various pressures, temperatures, hydrogen gas loadings or even during reactions with destabilizing agents. Ultimately, by *in-situ* diffraction we can study chemical reactions (for example de- and rehydrogenation) in more practical multicomponent mixtures, approaching the conditions of their anticipated technological use. The design and analysis of such complex systems requires the knowledge of the structure and properties of the fundamental H-rich component under various pressures and temperatures. Thus, bearing in mind the far-reaching research objectives, we will restrict ourselves here to the changes induced in light hydrides by the variation of the thermodynamic parameters, P and T.

2. Optimizing the Data Collection

From the point of view of crystallographic practice, solving and refining a new structure from excellent-quality high-pressure data measured at a synchrotron source is just like treating “bad” powder data, collected at ambient conditions with a standard laboratory source. The use of a small sample contained in a bulky sample environment inevitably reduces the quality of the diffraction data. Such datasets have a limited resolution both in the reciprocal (relatively broad peaks) and in the direct (limited 2θ range) space. Below is the list of tricks aiming to get the best high-pressure diffraction data from light hydrides.

- Most hydrides have relatively simple structures, giving preference to high-intensity medium-resolution area (2D) detectors over the high-resolution ones. The latter are needed only when there is a problem to index peaks of unknown structure or refine an occasionally complex structure, like $\text{Mg}(\text{BH}_4)_2$ (Černý *et al.*, 2007).

- Substances composed of the light elements give a weak diffraction signal and therefore a lower than usual signal-to-background ratio. The signal is even weaker for small light samples contained in a diamond anvil cell (DAC). Area detectors accumulate extremely high total intensity, thus reducing impact of statistical noise and providing a good time resolution. However, a long exposure time of >10 min. may be necessary to obtain good statistics for the high-angle peaks. For that, the low-background image plate detectors have an advantage over the CCDs.
- All spurious peaks coming from diamond, ruby (used for pressure calibration) etc. should be masked and removed before the integration into a 1D profile. “Cake” option in Fit2D should be used in order to verify the proper detector calibration. Diffraction rings of the sample can be used to determine the coordinates of the $2\theta = 0$ position and the detector tilts. The resulting 1D dataset will have the best resolution, which might be critical on the indexing stage.
- A pattern collected at low pressure, on a phase with a known structure, should be used for refining a “zero shift” value. This parameter has no physical meaning for area detectors, but it corrects for any small remaining calibration errors – this often helps to successfully index peaks of novel high-pressure phases.

On how to collect variable-temperature data at ambient pressure:

- Thin-walled glass capillaries give a relatively high amorphous background and react with some borohydrides at elevated T. A single-crystal sapphire capillary is an option to remove both undesired effects. Strong diffraction spots from the sapphire should be masked.
- In order to remove an uncertainty with non-ideal centering of a capillary, it should be rotated by the same angle and in the same angular range upon each exposure. In this case, the series of powder data collected sequentially at different temperatures will show a consistent (smooth) variation of the cell parameters. It will also allow using the same mask for all 2D images. A gas blower can be set to ramp up the temperature at a constant rate, with an automatic image retaking. This simple procedure reveals all temperature-induced changes in one run!

3. Solving Structures from Powder Diffraction Data

A combination of several programs proved to be very efficient in solving new structures. Their use will be illustrated during two workshops. Here the practical guidelines are given with only one case study, of LiBH₄. Thus, this chapter covers partly the lecture and the workshops.

- Input file for indexing in **Dicvol** can be generated and directly called from WinPlotr, a program shell of **FullProf**. Warning: zero shift in Dicvol is defined with the opposite sign to the one in FullProf. Avoid including peaks belonging to other phases: intensity variations for different peaks during heating or upon the compression help to reveal if they belong to the same phase. Be conservative: use only reliable peaks' positions. Indexing should be attempted up to the highest figures of merit (FOM). Other parameters to vary: EPS (expected error of peaks' positions) and the maximum unit cell volume.
- The resulting solutions should be analyzed by making a le Bail fit, also known as "profile matching". The correct cell should not predict too many peaks having zero observed intensity, unless the Bravais lattice is non-primitive. Program **ChekCell** and its subroutine **TrueCell** are the excellent tools for finding higher metric symmetry consistent with the list of indexed peaks, for finding a related supercell that explains extra weak peaks, and for finding a space group by an automated analysis of the systematic absences. The program requires as an input the cell parameters obtained by Dicvol and an extended list of peaks' positions, including the less reliable ones, which might belong to the same phase.
- An elegant trial and error method of structure solution is implemented in the program **FOX**. It works well with moderate-quality datasets, typically obtained at high pressures, where structure solution by direct methods (standard technique for single-crystal data) fails. The profile parameters and data for known secondary phases should be transferred to FOX from the le Bail fit. A few datasets can be used simultaneously.
- The great advantage of the direct space structure solution is the possibility to add our knowledge or expectations of the structural behavior, thus reducing the space of the optimized parameters. The crystal chemistry can be defined in FOX via a set of antibump restraints (minimum distances between atoms of various types) and by defining rigid or semi-rigid bodies. For example, BH₄ groups can be located as complete tetrahedral units, first optimizing only three positional parameters and on the final stage also three orientational parameters. Compared to five independent atoms (15 parameters), this gives a considerable reduction in the number of free parameters. Also, FOX does not require an exact composition: provided the atoms types are correct and given in access to the expected composition, the structure will be solved, and the excess atoms eliminated by using so called "dynamic occupancy correction".
- Once an input file for FOX is generated, structure solution can be easily attempted in different space groups – it is a matter of changing the space group only. With sufficient amount of the empirical information put in, the search limits may be sufficiently narrowed, enabling even the

structure solution in the triclinic space groups. This may allow solving a structure without guessing the space group. The true symmetry can be revealed later by analyzing the resulting “triclinic” structure.

- For the successful structure solution of some new phases forming in DACs, it is essential to model a texture, by including one parameter (March’s model) into the global optimization by FOX. Various directions of the preferred orientation should be tested, e.g. for the orthorhombic cell the three main axes should be tested as possible directions. Another approach (*Whitfield*, 2009) does not require an input of the orientation direction when using spherical harmonics preferred orientation correction during the simulated annealing in TOPAS. The remarkable feature of the preferred orientation developing in DACs is the uniform distribution of the diffraction intensities along the Debye rings. In the experimental geometry, where the compression direction coincides with the direction of the primary beam and the area detector is put at $2\theta = 0$ position, the texture appears visually undetectable. Indeed, Figure 1 shows that the powder is averaged by rotation around the axis of the primary beam, thus forming regular powder rings but leaving the perpendicular direction unique. Thus, when all attempts to solve a structure fail, the texture should be assumed *a priori*, making it a part of the globally optimized model (*Filinchuk et al.*, 2007). Certainly, this is the option of the last resort.
- A possibly higher crystallographic symmetry of the structure obtained with FOX can be detected in the program **Platon**, using ADDSYM routine. In particular, it enables finding the true symmetry for structures solved in the triclinic space groups. An automatic search for unoccupied voids (CALC VOID) helps to reveal physically unrealistic cavities which usually indicate that some atoms are missing. Once the major part of the structure is identified, the structure can be completed using difference Fourier maps: they can be calculated both in FOX and in FullProf. Amusingly, there are rare cases of truly empty voids in largely ionic borohydrides, see $\text{Mg}(\text{BH}_4)_2$ as an example (*Filinchuk et al.*, 2009).
- Generation of distorted variants of the known structure types can not be considered as an *ab initio* structure solution, but it is often a way to describe new lower-symmetry derivatives of the known parent structures. For example, an appearance of extra peaks or peaks’ splitting upon a phase transition might be explained by a superstructure. The possible superstructures can be generated using group–subgroup relations implemented in **PowderCell**. Small distortions can be introduced manually in the resulting trial models, and the simulated powder patterns can be compared to the experimental ones in order to confirm or reject these variants. Unfortunately, this program does not generate subgroups of the space groups in the non-standard settings – the full list can be found in

the International Tables, volumes A and A1. Sometimes, the symmetry lowering does not proceed via the Γ -point (group–subgroup), but goes via more complicated mechanisms involving other points of the Brillouin zone. Investigating such possibilities requires making a group-theoretical analysis, which can be easier to do employing the **Bilbao Crystallographic Server**.

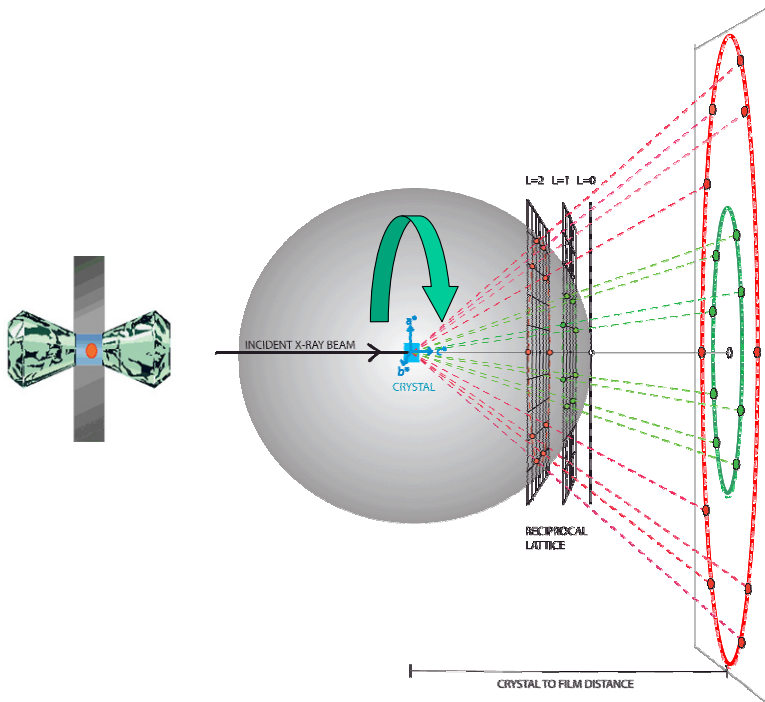


Figure 1. Typical diffraction geometry of the high-pressure experiment in a DAC provides a good powder average by rotation around the axis of the primary beam, forming uniform Debye rings, but leaves the perpendicular direction unique. The texture along this direction is visually undetectable.

- The resulting structure should be finally refined by **Rietveld method**, using, for example, FullProf. A correct weighting scheme should be used in order to obtain unbiased refined parameters. For this, the 2θ – intensity data should be complemented by a third column containing uncertainties of the integrated intensities, $\sigma(I)$. The resulting large χ^2 values should not come at a surprise, since a statistically small difference between the observed and theoretical patterns cannot be practically achieved in the presence of a vanishingly small noise – any small difference will be considered as statistically significant.

- In cases when a structure shows unexpected features, **DFT calculations** can be used as a part of the structure validation: a DFT-optimization of the experimental structure should converge at nearly the same configuration. Theoretical calculations can also be used to discriminate between a few structures showing a similar fit to the diffraction data: the lowest energy structure is most likely the true one. It is interesting that theoretical predictions of crystal structures of hydrides typically fail. All new compositions and crystal structures have been discovered yet in experiments. Light hydrides seem to be a challenge for theory due to the pronounced rotational dynamics of the light isolated groups, such as BH_4 , and the related contribution of the entropy to the total energy. These complications are illustrated by the example of LiBH_4 (*Filinchuk et al.*, 2008a, c).
- A symmetry-based phenomenological analysis of the structures observed under various P–T conditions helps to understand atomistic mechanisms and thermodynamic aspects of the phase transitions (see *Dmitriev et al.*, 2008 as an example). The **symmetry-based analysis** combined with the powder diffraction experiment allows to construct the pressure–temperature phase diagram and even to go beyond making predictions of new possible phases.

4. A Case Study – LiBH_4

Theoretical predictions of the high-pressure phases of LiBH_4 did not explain the observed powder pattern, collected at 2.4 GPa. None of the known structure types of the ABX_4 family could be matched with our diffraction data, thus the structure had to be solved *ab initio* (Figure 2). The peaks were indexed using Dicvol in a tetragonal cell with $a \sim 3.75$ and $c \sim 6.45$ Å, however the structure could not be solved in any of the tetragonal space groups. It has therefore been solved by global optimization in direct space (program FOX) in the lowest symmetry space group *P1*. Constraints on tetrahedral symmetry of the borohydride anion have been imposed, along with soft “antibump” restraints on $\text{Li} \dots \text{H}$ distances. The true symmetry of the resulting structure has been uncovered using Platon software, which suggested a doubled pseudo-tetragonal cell ($a, b \sim 5.30$ and $c \sim 6.45$ Å) and the orthorhombic space group *Ama2*. Thus, it was the pseudo-tetragonal metrics of the orthorhombic structure that made the structure solution so intricate. Fortunately, there was no effect of texture.

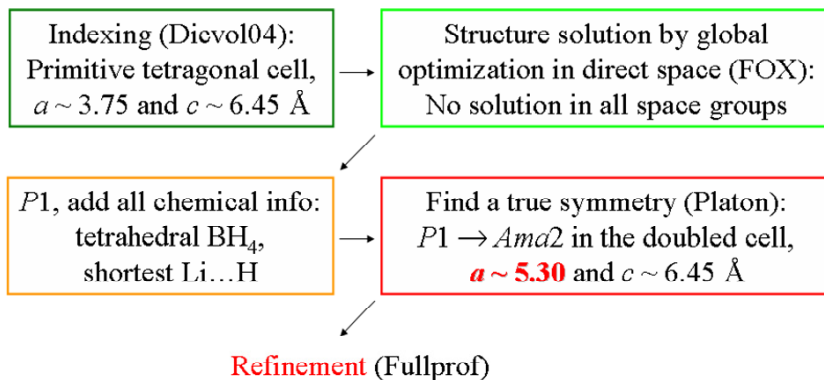


Figure 2. The sequence of steps made for solving the structure of the high-pressure phase of LiBH_4 (Filinchuk *et al.*, 2008c).

This model was refined by the Rietveld method, keeping the z -coordinate for the Li atom fixed to zero (in order to fix the origin of the polar space group). 47 reflections were fitted with 11 intensity-dependent parameters, using eight soft restraints defining an approximately tetrahedral BH_4^- geometry. This approach provided a very good fit to the data using a minimal set of reasonable assumptions.

The $\text{Ama}2$ phase reveals a new structure type. BH_4^- anions form a distorted Cu-type substructure, while Li atoms form a primitive cubic substructure (α -Po-type). The Li and BH_4^- sublattices interpenetrate, so that Li atoms occupy tetrahedral voids in the BH_4^- network. Most interestingly, the BH_4^- anion has a nearly square planar coordination by four Li atoms (Figure 3) – a square coordination of BH_4^- anions has no analogues in the crystal chemistry of metal borohydrides (Filinchuk *et al.*, 2008b).

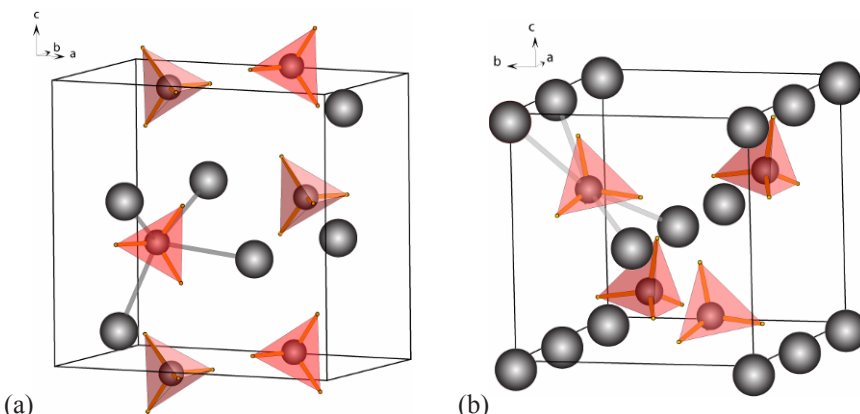


Figure 3. Crystal structures of the LiBH_4 phases observed at 0–1 GPa (left) and 1–10 GPa (right) at ambient temperature. At higher temperatures a hexagonal, and at higher pressures – a cubic phases appear (not shown here).

To validate the structure and gain insight into stability of the novel coordination of BH_4^- by metal atoms, the density functional theory (DFT) calculations were employed. The optimized structure is in good agreement with the experimental one: the BH_4^- anion fits exactly into the plane of Li neighbors, compared to its small deviation from the plane in the experimental structure. This gives more confidence in the novel planar coordination of the BH_4^- unit.

In the *Ama2* phase, the shortest H...H distance between two neighboring BH_4^- anions is 1.87 Å long in the theoretically optimized model, which is even shorter than 1.92 Å obtained from the crystallographic data. These short contacts serve as links within chains formed by borohydride anions, as shown in Figure 4. This geometry is unique, and so short an H...H distance is unprecedented in metal borohydrides. The short inter-anionic contact H...H correlates with the more acute H–B–H angle of $\sim 102^\circ$ in the DFT-optimized structure (compared with 109.5° for ideal tetrahedral geometry). One can say that the H...H interactions distort the BH_4^- anion, and such a distortion is supposed to be a step towards a decomposition of BH_4^- .

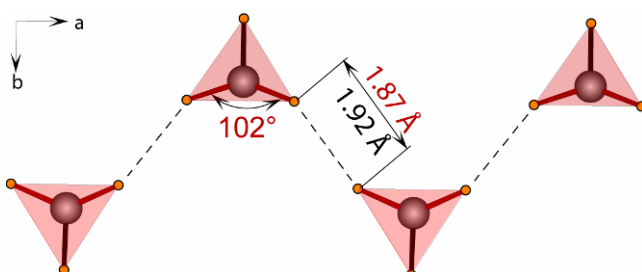


Figure 4. In the *Ama2* phase of LiBH_4 the BH_4^- anions are linked by short H...H contacts into chains. These interactions distort the otherwise tetrahedral BH_4^- anion.

Short H...H interaction are likely to decrease the activation energy for hydrogen desorption. Thus, this structure may show completely different hydrogen storage properties if stabilized by chemical substitution at ambient pressure. It was suggested that the internal pressure in the structure may be tuned by a partial substitution of lithium by larger cations, or substitution of some BH_4^- groups by AlH_4^- or halide anions. The resulting LiBH_4 -based substance with *Ama2* structure may show more favorable hydrogen storage properties than pure LiBH_4 and may turn out to be useful for hydrogen storage applications.

All together, at different P–T conditions, four LiBH_4 phases are known: two at ambient and two at high pressure. The low-temperature structure has the *Pnma* symmetry. It transforms into a hexagonal *P6₃mc* wurtzite-like high-temperature phase at ~ 380 K. At pressures above 10 GPa a cubic phase

forms. *In situ* synchrotron diffraction serves as an optimal probe to map out the P-T diagram (Figure 5), identify the phases and follow their structural evolution. Such a diagram, with all the supporting information, allows evaluation of fundamental thermodynamic and structural properties of LiBH₄.

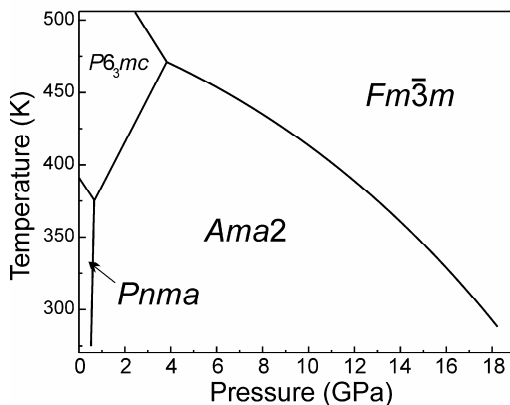


Figure 5. Experimental pressure-temperature phase diagram of LiBH₄.

An analysis of symmetry changes and structural deformations, followed by a group theoretical analysis, yields a unified picture of the phase transformations in LiBH₄. An existence of cation-anion layers in all four LiBH₄ phases is suggested from the phenomenological analysis of mechanisms of phase transitions. A clear evidence for the existence of cation-anion layers is found in the hexagonal phase, where the BH₄ tetrahedron has three short B...Li contacts in the *ab* plane and a long one along the *c* axis. In the *Pnma* phase, these layers are corrugated and the structure is less anisotropic. The layers where Li and BH₄ groups are associated by means of the shorter B...Li contacts can be identified in the (011) plane of the *Ama2* structure. In the cubic phase, one type of layer is consistent both with geometrical considerations and with the phenomenological model: these are cation-anion layers situated in the (111) plane, similar to those found in the hexagonal phase. Clearly, the formation of layers in the LiBH₄ structures is not determined by coordination polyhedra for Li and BH₄ groups, since corresponding coordination numbers and geometries vary with pressure and temperature. Directional interaction of tetrahedral BH₄ with spherical metal atoms explains the relative complexity of LiBH₄ structures and of the P-T phase diagram in comparison with NaCl, where both cation and anion are spherical.

References

- Černý R., Filinchuk Y., Hagemann H., Yvon K. (2007) *Angew. Chem. Int. Ed.* **46**, 5765.
- Dmitriev V., Filinchuk Y., Chernyshov D., Talyzin A.V., Dzwilewski A., Andersson O., Sundqvist B., Kurnosov A. (2008) *Phys. Rev. B* **77**, 174112.
- Filinchuk Y., Talyzin A.V., Chernyshov D., Dmitriev V. (2007) *Phys. Rev. B* **76**, 092104.
- Filinchuk Y., Černý R., Hagemann H. (2009) *Chem. Mater.* **21**, 925.
- Filinchuk Y., Chernyshov D., Černý R. (2008a) *J. Phys. Chem. C* **112**, 10579.
- Filinchuk Y., Chernyshov D., Dmitriev V. (2008b) *Z. Kristallogr.* **223**, 649.
- Filinchuk Y., Chernyshov D., Nevidomskyy A., Dmitriev V. (2008c) *Angew. Chem. Int. Ed.* **47**, 529.
- Whitfield P. S. *J. Appl. Cryst.* **42** (2009) 134.